DALTON
FULL PAPER

Supramolecular assemblies from ditopic ligands and transition metal salts †

Hamish A. Miller, Norman Laing, Simon Parsons, Andrew Parkin, Peter A. Tasker * and David J. White

Department of Chemistry, The University of Edinburgh, Joseph Black Building, Kings Buildings, West Mains Road, Edinburgh, UK EH9 3JJ. E-mail: p.a.tasker@ed.ac.uk

Received 28th April 2000, Accepted 7th June 2000
First published as an Advance Article on the web 20th September 2000

Tetradentate salicylaldimine ligands of the H_2salen-type bearing *ortho*-*N*-morpholinomethyl substituents function as ditopic ligands, bonding to Ni^{II} or Cu^{II} with the $[N_2O_2]^{2-}$ donor set of the salen unit and a sulfate or two nitrate anions with the protonated morpholine units. The binding of the metal salt by the zwitterionic form of the ligand provides a novel approach to the transport of metal sulfates in metal recovery processes. A comparison of the solid state structures of a "free" ligand with a series of nickel(II) complexes demonstrates that the metal ion templates the ligand system, orientating the pendant morpholinium groups to form electrostatic and bifurcated hydrogen bonds in the sulfate complex to the dianion creating a neutral 1 : 1 : 1 $[LM^{2+}X^{2-}]$ complex suitable for extraction into water immiscible solvents. Other binding modes involving bridging of metal complex units by anion binding to the pendant morpholine groups suggest that these ditopic ligands could also be used to assemble unusual three-dimensional arrays of metal complexes in the solid state.

Introduction

Many man-made processes to separate metal ions and recover metals from aqueous solution depend on ion exchange processes[1] in which the desired cation M^{n+} replaces a different metal cation (often Na^+) or protons from an anionic group in a complexing agent. Such agents may be deployed on a solid support in processes using ion exchange resins or in a water immiscible liquid in solvent extraction, eqn. (1). While such processes

$$\overline{n\mathrm{HL}} + \mathrm{M}^{n+} \rightleftharpoons \overline{\mathrm{ML}_n} + n\mathrm{H}^+ \qquad (1)$$

are well suited to a number of flowsheets used to recover metals from both primary and secondary sources, there are situations when a much more efficient approach is to transport metal *salts*. Such an approach requires complexing agents which accommodate both the metal cation and its attendant anion(s). This paper addresses the design of ditopic ligands, which can reversibly transfer metal salts from aqueous feed solutions as in eqn. (2).

$$\overline{\mathrm{L}} + \mathrm{M}^{n+} + \mathrm{X}^{n-} \rightleftharpoons \overline{\mathrm{MLX}} \qquad (2)$$

A "proton-swing" controlled loading and stripping of metals, as in eqn. (1), is ideal for the recovery of metals from oxidic ores using the flowsheet outlined in Fig. 1 for the recovery of copper from "heap leach/solvent extraction/electrowinning" operations.[2] The crude metal sulfate solution obtained by initial acid leaching of the ore is contacted with an organic phase containing the lipophilic ligand, selectively extracting the metal ion and releasing two protons into the aqueous phase. A pure metal sulfate solution can then be obtained by stripping the organic phase with stronger sulfuric acid than that present in the pregnant leach solution. This pH gradient provides the driving force across the circuit. In the final stage electrolysis (or "electrowinning") is used to obtain the pure metal.

An excellent overall materials balance is obtained because the acid consumed in leaching the oxide is replaced in the extraction step and the organic extractant, HL, is regenerated by stripping the metal with acid generated in the electrowinning process. This feature has underpinned the remarkable growth in the last decade of solvent extraction technology, which now accounts for more than 20% of copper production worldwide. Whilst ion-exchange extractants are well suited to circuits for processing oxidic and related "transition" ores they cannot provide a good materials balance for hydrometallurgical treatment of sulfidic ores or for the recovery of metals from many secondary sources or effluents such as acid mine drainage streams. Pressure or bacterial leaching of sulfides does not consume acid (Fig. 2). Consequently, if the conventional types of acidic reagents are used in the extraction process, sulfuric acid would build up at the front end of the circuit, requiring neutralisation which will generate a salt waste which will have to be removed to allow recycling of the leachate. This problem could be overcome using reagents, which would transport the desired metal as its sulfate salt across a leach/solvent extraction/electrowin circuit as in Fig. 2. Neutralisation of acid is now only required to control the pH of the electrolyte at the back end of the circuit.

Transport of metal salts as in eqn. (2) requires reagents with an affinity for both the metal cation and its attendant anion. The systematic development of anion complexing agents[3] has been the subject of much work recently. Selective binding of anions often involves a suitable arrangement of hydrogen bond donors such as amides, sulfonamides or (thio)ureas which can be either neutral or cationic.[4] Positively charged anion receptors usually contain protonated nitrogen atoms or metal ions. A number of researchers have exploited these developments to obtain organic ligands designed to bind a combination of a metal cation and its attendant anion,[5] either by incorporating separate cation or anion binding sites into a single ligand or by

† Based on the presentation given at Dalton Discussion No. 3, 9–11th September 2000, University of Bologna, Italy.

Electronic supplementary information (ESI) available: rotatable 3-D crystal structure diagram in CHIME format. See http://www.rsc.org/suppdata/dt/b0/b003436n/

DOI: 10.1039/b003436n

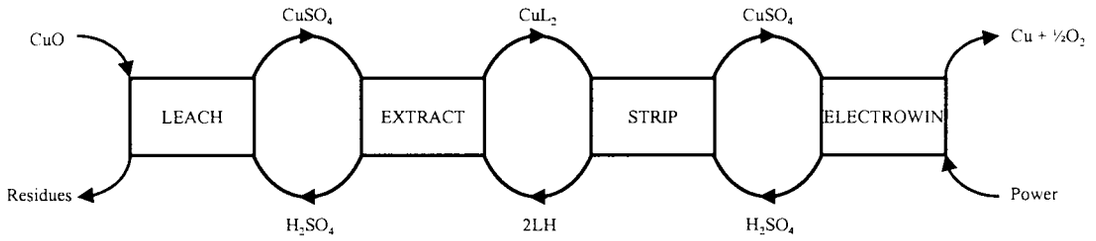

$CuO + H_2SO_4$	$\rightleftharpoons$	$\overline{CuSO_4} + H_2O$	Leach
$CuSO_4 + 2\overline{LH}$	$\rightleftharpoons$	$\overline{CuL_2} + H_2SO_4$	Extract
$\overline{CuL_2} + H_2SO_4$	$\rightleftharpoons$	$CuSO_4 + 2\overline{LH}$	Strip
$CuSO_4 + H_2O$	$\rightleftharpoons$	$Cu + ½O_2 + H_2SO_4$	Electrowin
CuO	$\rightleftharpoons$	$Cu + ½O_2$	Overall

Fig. 1 The flowsheet and materials balance for recovery of copper from oxidic tailings using sulfuric acid heap leaching, solvent extraction with phenolic oxime reagents and electrowinning in a conventional tankhouse.

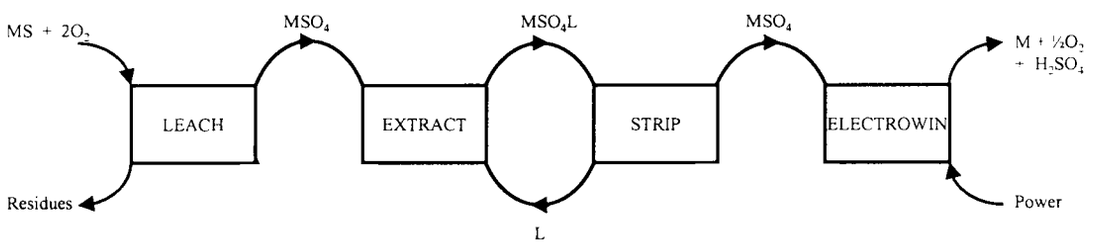

$MS + 2O_2$	$\rightleftharpoons$	$\overline{MSO_4}$	Leach
$MSO_4 + \overline{L}$	$\rightleftharpoons$	$\overline{MLSO_4}$	Extract
$\overline{MLSO_4}$	$\rightleftharpoons$	$MSO_4 + \overline{L}$	Strip
$MSO_4 + H_2O$	$\rightleftharpoons$	$M + ½O_2 + H_2SO_4$	Electrowin
$MS + H_2O + 1½O_2$	$\rightleftharpoons$	$M + H_2SO_4$	Overall

Fig. 2 A proposed flowsheet and materials balance for recovery of metals from sulfidic ores using pressure leaching, solvent extraction with metal salt transportation and electrowinnning.

arranging for the anion to interact directly with the metal centre *via* a vacant co-ordination site.[6]

Of particular interest to us are those molecules or mixtures of molecules capable of transporting metal ions and their attendant anions in liquid/liquid extractions or across membranes. Beer *et al*. have developed a tripodal tris(amidobenzo-15-crown-5) ditopic ligand to extract technetium as the [Na][TcO_4] ion pair.[7] Kavallieratos *et al.* enhanced the extraction of $CsNO_3$ by tetrabenzo-24-crown-8 by the addition of benzene-1,3,5-tricarboxamide which formed hydrogen bonds to the nitrate ion.[8] Similarly, Unguro and co-workers have used mixtures of anion and cation binders to transport CsCl and KCl across membranes. These researchers also covalently linked anion and cation binding moieties into a single molecule capable of metal salt transport.[9]

This paper describes some relatively simple ditopic ligands derived from H_2salen, which have been designed[10] to effect the transport of metal sulfates in a circuit of the type shown in Fig. 2. A key design feature of these ligands is that the metal salt is bound in a zwitterionic form of the ligand (Scheme 1). This will permit sequential stripping of the cation and anion as shown, recycling the ligand and generating a concentrated metal sulfate solution for electrowinning and ammonium sulfate as a saleable product. The prototype ligand (Scheme 2) contains an $[N_2O_2]^{2-}$ donor set and two pendant tertiary amine groups (morpholines) designed to capture the two phenolic protons liberated upon metal binding, thus forming a dicationic binding site for

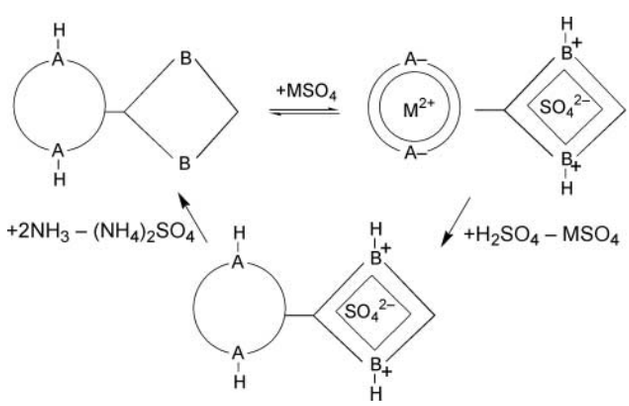

Scheme 1 Representation of ditopic ligands for metal sulfates with diacid/dibasic sites to enable the hydrometallurgical unit operations of concentration and separation.

the anion(s). Selection of different bridging groups (R), alkyl substituents (R′) on the phenol and pendant amine functionalities allows fine-tuning of the strength and selectivity of complex formation and solubility and phase engagement properties of the extractant.

In this paper crystal structure determinations of nickel(II) complexes of ligand **1** and of a "free" ligand **2** (Scheme 3) are used to establish the mode of anion binding and to account for the assembly of extractable metal salt complexes. The impli-

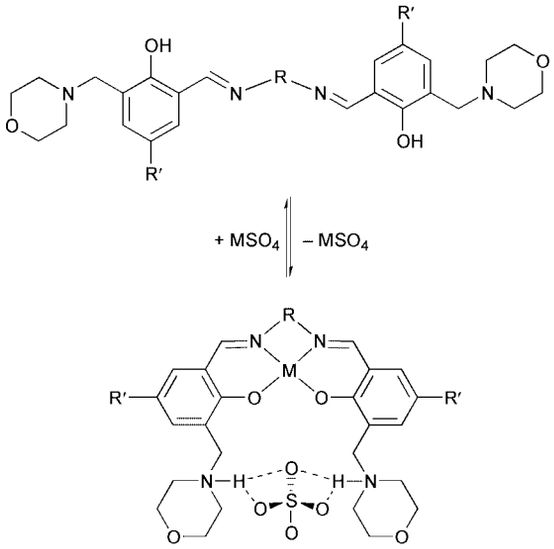

Scheme 2 Sequestration of a divalent transition metal sulfate.

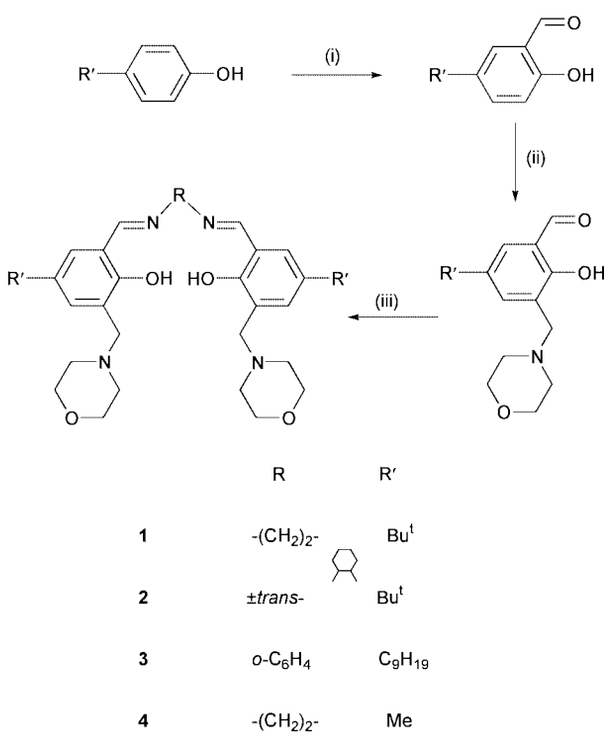

Scheme 3 (ia) MgOMe, MeOH–toluene, reflux 3 h; (ib) paraformaldehyde, distillation; (ii) ethoxymorpholinomethane, MeCN, N_2, reflux 66 h; (iii) diamine, Et_2O–EtOH (1 : 1), r.t. 24 h.

cations of using a templating role of the metal and the strong anion binding sites to assemble tailor made three-dimensional arrays of metal complex units are also considered briefly.

Experimental

Instrumentation

Nuclear magnetic resonance spectra were obtained on Bruker AC 200 and AC 250 instruments, FAB mass spectra on a Kratos MS 50 machine, EI mass spectra on a Kratos Profile instrument, FTIR spectra on a Perkin-Elmer Paragon 1000 spectrometer as dichloromethane films on NaCl plates or as KBr discs and electronic absorption spectra on a Unicam UV2 spectrometer. Magnetic susceptibly measurements were carried out on a Johnson Mathey magnetic susceptibility balance and molar susceptibilities were corrected for diamagnetism using Pascal's constants.[11] Inductively coupled plasma atomic emission spectroscopy (ICP-EAS) analysis was performed on a Thermo Jarrell Ash IRIS ICP-EAS spectrometer.

Solvent and reagent pre-treatment

Unless stated to the contrary commercial grade chemicals obtained from Aldrich or Acros companies were used without further purification.

Ligand synthesis

The 5-alkyl-2-hydroxybenzaldehydes and ethoxymorpholinomethane were prepared by the methods described by Levin and co-workers[12] and Fenton and co-workers.[13] The salicylaldehydes substituted with pendant morpholino groups were prepared by an adaptation of the method of Fenton and co-workers[13] as follows.

5-*tert*-Butyl-2-hydroxy-3-(morpholinomethyl)benzaldehyde. A mixture of 5-*tert*-butylbenzaldehyde (14.8 g, 0.1 mol) and ethoxymorpholinomethane (15.95 g, 0.11 mol) in acetonitrile (200 cm^3) was heated to reflux under a dinitrogen atmosphere for 72 h. After cooling to room temperature the solvent was removed *in vacuo* to yield a viscous light green oil. The product was dissolved in CH_2Cl_2 (150 cm^3) and extracted with water (3 × 60 cm^3). The organic fraction was evaporated *in vacuo* and dried under vacuum (27.23 g, 98%). Found: C, 69.07; H, 8.54; N, 5.14. Calc. for $C_{16}H_{23}NO_3$: C, 69.29; H, 8.36; N, 5.05%. δ_H ($CDCl_3$, 200 MHz) 1.28 (s, 9 H, $C(CH_3)_3$), 2.55 (t, *J* 4.6, 4 H, NCH_2CH_2O), 3.69 (s, 2 H, CH_2N), 3.75 (t, *J* 4.6, 4 H, NCH_2CH_2O), 7.37 (d, 1 H, *J* 2.6, Ar H), 7.59 (d, 1 H, *J* 2.6 Hz, Ar H) and 10.24 (s, 1 H, ArC*H*O). δ_C ($CDCl_3$) 31 (CH_3), 34 ($C(CH_3)_3$), 53 (NCH_2CH_2O), 59 (CCH_2N), 67 (NCH_2CH_2O), 88 (Ar C), 126 (Ar C), 131 (Ar CH), 133 (Ar CH), 159 (Ar C), 157 (Ar C) and 193 (ArC*H*O). MS (FAB, thioglycerol): *m*/*z* 278 (MH^+, 17%).

2-Hydroxy-3-(morpholinomethyl)-5-nonylbenzaldehyde. A mixture of 5-nonylbenzaldehyde (28.4 g, 0.1 mol) and ethoxymorpholinomethane (15.95 g, 0.11 mol) in acetonitrile (200 cm^3) was heated to reflux under a dinitrogen atmosphere for 96 h. After cooling to room temperature the solvent was removed *in vacuo* to yield a viscous light green oil. The product was dissolved in CH_2Cl_2 (150 cm^3) and extracted with water (3 × 60 cm^3). The organic fraction was evaporated *in vacuo* and dried under vacuum (34.6 g, 99%). The product was used without further purification (Found: C, 71.95; H, 9.39; N, 4.00. Calc. for $C_{21}H_{33}NO_3$: C, 72.59; H, 9.57; N, 4.03%). δ_H ($CDCl_3$, 200 MHz) 0.42–1.70 (m, 19 H, C_9H_{19} mixed isomer chain), 2.54 (m, 4 H, NCH_2CH_2O), 3.68 (s, 2 H, CH_2N), 3.74 (m, 4 H, NCH_2CH_2O), 7.35 (d, 1 H, *J* 2.3, Ar H), 7.51 (d, 1 H, *J* 2.3 Hz, Ar H) and 10.62 (s, 1 H, ArC*H*O). δ_C ($CDCl_3$) 8–52 (C_9 mixed isomer chain), 53 (NCH_2CH_2O), 59 (CCH_2N), 67 (NCH_2CH_2O), 121 (Ar C), 123 (Ar C), 127 (Ar CH), 135 (Ar CH), 139 (Ar *C*), 158 (Ar *C*) and 193 (ArC*H*O). EIMS: *m*/*z* 347 (M^+, 26%).

Ligand 1. 5-*tert*-Butyl-2-hydroxy-3-(morpholinomethyl)benzaldehyde (6 g, 21.7 mmol) was dissolved in diethyl ether (60 cm^3) and added to a solution of ethane-1,2-diamine (0.636 g, 10.6 mmol) in ethanol (60 cm^3). The resulting yellow solution was stirred overnight then concentrated *in vacuo* to give a yellow oil which on trituration in hexane at −78 °C gave a waxy yellow solid. This was washed with hexane (15 cm^3) and diethyl ether (15 cm^3) and dried *in vacuo* (5.8 g, 95%), mp 155–158 °C (Found: C, 70.60; H, 9.06; N, 9.67. Calc. for $C_{17}H_{25}N_2O_2$: C, 70.56; H, 8.71; N, 9.68%). λ_{max}/nm (CH_2Cl_2) 235, 262, 329 and 413. δ_H ($CDCl_3$, 200 MHz) 1.28 (s, 9 H, $C(CH_3)_3$), 2.50 (t, *J* 4.6, 4 H, NCH_2CH_2O), 3.58 (s, 2 H, NCH_2CH_2N), 3.71 (t, *J* 4.6, 4 H, NCH_2CH_2O), 3.90 (s, 2 H, Ar CH_2N), 7.14 (d, 1 H, *J* 2.5, Ar H), 7.37 (d, 1 H, *J* 2.5 Hz, Ar H), 8.37 (s, 1 H, N=CH) and 13.23 (s, br, 1 H, OH). δ_C ($CDCl_3$) 31 (CH_3), 34 ($C(CH_3)_3$), 53 (NCH_2CH_2O), 57 (CCH_2N), 60 (NCH_2CH_2N), 67 (NCH_2-

CH_2O), 118 (Ar C), 124 (Ar C), 127 (Ar CH), 131 (Ar CH), 141 (Ar C), 157 (Ar C) and 167 (CHN). MS (FAB, thioglycerol): *m*/*z* 579 (MH^+, 62%).

Ligand 2. This was prepared similarly from 5-*tert*-butyl-2-hydroxy-3-(morpholinomethyl)benzaldehyde and ±*trans*-cyclohexane-1,2-diamine. The yellow product was recrystallised from hexane, collected by filtration and air-dried (1.080 g, 74%), mp 103–106 °C (Found: C, 72.99; H, 9.64; N, 7.94. Calc. for $C_{38}H_{56}N_4O_4\cdot\frac{1}{2}C_6H_{14}$: C, 72.85; H, 9.33; N, 8.29%). λ_{max}/nm (CH_2Cl_2) 234, 261, 328 and 417. δ_H ($CDCl_3$, 200 MHz) 1.23 (s, 9 H, C(CH_3)$_3$), 1.66 (m, br, 4 H, cyclohexane CH_2), 1.86 (m, br, 4 H, cyclohexane CH_2), 2.48 (t, *J* 4.5, 4 H, NCH_2CH_2O), 3.30 (m, 1 H, cyclohexane NCH), 3.70 (t, *J* 4.5, 4 H, NCH_2CH_2O), 3.54 (s, 2 H, Ar CH_2N), 7.06 (d, 1 H, *J* 2.4, Ar H), 7.33 (d, 1 H, *J* 2.4 Hz, Ar H), 8.27 (s, 1 H, N=CH) and 13.5 (s, br, 1 H, OH). δ_C ($CDCl_3$) 24.07 (cyclohexane C), 31.23 (CH_3), 31.43 (cyclohexane C), 33.70 (C(*C*H_3)$_3$), 53.08 (C*C*H_2N), 53.57 (N*C*H_2-CH_2O), 56.65 (cyclohexane C), 59.58 (cyclohexane C), 66.84 (NCH_2*C*H_2O), 117.6 (Ar C), 124.0 (Ar C), 127 (Ar CH), 131 (Ar CH), 141 (Ar C), 157 (Ar C) and 165 (CHN). MS (FAB, thioglycerol): *m*/*z* 633 (MH^+, 42%).

Ligand 3. This was similarly prepared from 2-hydroxy-3-(morpholinomethyl)-5-nonylbenzaldehyde and benzene-1,2-diamine. The crude product was isolated as a viscous oil, dissolved in chloroform (200 cm^3) and extracted with water (3 × 100 cm^3). The chloroform solution of **3** was isolated, evaporated to dryness and the product dried *in vacuo* to yield a highly viscous yellow oil (3.07 g, 82%). The product was used without further purification in solvent extraction experiments (Found: C, 67.19; H, 8.25; N, 6.90. Calc. for $C_{48}H_{70}N_4O_4\cdot CHCl_3$: C, 66.39; H, 8.07; N, 6.32%). δ_H ($CDCl_3$, 200 MHz) 0.5–1.69 (m, 19 H, C_9H_{19} mixed isomer chain), 2.53 (m, 4 H, NCH_2CH_2O), 3.72 (m, 6 H, OCH_2CH_2N + Ar CH_2N), 6.77 (m, 1 H, Ar H), 7.07 (m, 1 H, Ar H), 7.24–7.37 (m, 2 H, Ar H), 8.65 (s, 1 H, CH=N) and 13.50 (br, 1 H, OH). δ_C ($CDCl_3$) 10–63 (C_9 mixed isomer chain), 52.8 (N*C*H_2CH_2O), 66.60 (NCH_2*C*H_2O), 66.70 (C*C*H_2N), 110.4 (Ar C), 114.6 (Ar C), 115.5 (Ar C), 118.1 (Ar C), 118.5 (Ar CH), 119.0 (Ar CH), 119.6 (Ar CH), 122.2 (Ar CH), 123.5 (Ar C), 127.2 (Ar CH), 127.7 (Ar CH), 153.6 (Ar C) and 157.3 (CHN). MS (FAB, thioglycerol): *m*/*z* 768 (MH^+, 90%).

Preparation of complexes of metal salts

A solution of ligand (0.3 mM) in methanol (20 cm^3) was stirred together with a solution of the appropriate metal salt MX_n (1 mol equivalent) in methanol (20 cm^3) overnight. Colour changes due to complex formation were instantaneous. After removal of the solvent *in vacuo* the products were recrystallised as indicated and air-dried.

[Ni(1)(SO$_4$)], MX$_n$ = NiSO$_4$·6H$_2$O. Recrystallisation from MeOH–water 3:1 gave a red microcrystalline material formulated as [Ni(**1**)(SO$_4$)]·6H$_2$O (0.59 g, 93.6%), mp 235–240 °C (Found: C, 48.86; H, 7.37; N, 6.53. Calc. for $C_{34}H_{62}N_4NiO_{14}S$: C, 48.53; H, 7.43; N, 6.66%). $\chi_m = 1.14 \times 10^{-9}$ cm^3 mol^{-1}, $\mu_{eff} = 1.7 \times 10^{-3}$ μ_B. δ_H ($CDCl_3$, 200 MHz) 1.27 (m, 9 H, C(CH_3)$_3$), 2.6–3.3 (br, 4 H, NCH_2CH_2O), 3.49 (s, 2 H, NCH_2CH_2N), 3.7–4.2 (br, 4 H, NCH_2CH_2O), 4.3 (s, 2 H, Ar CH_2N), 7.21 (d, 1 H, *J* 2.5, Ar H), 7.29 (d, 1 H, *J* 2.5 Hz, Ar H) and 7.67 (s, 1 H, N=CH). MS (FAB, thioglycerol): *m*/*z* 733 (MH^+, 10%). λ_{max}/nm (CH_2Cl_2) 328, 339, 418 and 460 (sh). $\tilde{\nu}_{max}$/cm^{-1} 1119vs (SO_4). Crystals suitable for X-ray diffraction were obtained by evaporation of a saturated methanol solution of the complex.

[Ni(1)(NO$_3$)$_2$], MX$_n$ = Ni(NO$_3$)$_2$·6H$_2$O. Recrystallisation from diethyl ether gave an orange-red microcrystalline powder formulated as [Ni(**1**)(NO$_3$)$_2$]·3H$_2$O (0.253 g, 91%), mp 200–204 °C (Found: C, 49.79; H, 6.35; N, 10.76. Calc. for $C_{34}H_{56}N_6NiO_{13}$: C, 50.11; H, 6.88; N, 10.31%). $\chi_m = 2.11 \times 10^{-10}$ cm^3 mol^{-1}, $\mu_{eff} = 7.0 \times 10^{-4}$ μ_B. δ_H ($CDCl_3$, 200 MHz) 1.24 (m, 9 H, C(CH_3)$_3$), 3.21 (br, 4 H, NCH_2CH_2O), 3.45 (s, 2 H, NCH_2-CH_2N), 3.91 (br, 4 H, NCH_2CH_2O), 4.23 (s, 2 H, Ar CH_2N), 7.22 (d, 1 H, *J* 2.1, Ar H), 7.49 (d, 1 H, *J* 2.1 Hz, Ar H) and 7.65 (s, 1 H, N=CH). λ_{max}/nm (CH_2Cl_2) 327, 339, 415 and 460 (sh). $\tilde{\nu}_{max}$/cm^{-1} 1366vs and 1398vs (NO_3). MS (FAB, thioglycerol): *m*/*z* 699 (MH^+, 4%). Dissolving the material in dichloromethane and layering with hexane produced single crystals suitable for X-ray diffraction.

[Cu(1)(SO$_4$)], MX$_n$ = CuSO$_4$·5H$_2$O. Recrystallisation from EtOH–ether gave a dark brown crystalline material formulated as [Cu(**1**)(SO$_4$)]·5H$_2$O (0.111 g, 43%), mp 268–270 °C (Found: C, 51.96; H, 7.05; N, 6.33. Calc. for $C_{34}H_{60}CuN_4O_{13}S$: C, 52.44; H, 7.77; N, 6.80%). λ_{max}/nm (CH_2Cl_2) 371 and 557. $\tilde{\nu}_{max}$/cm^{-1} 1119vs (SO_4). MS (FAB, thioglycerol): *m*/*z* 734 (MH^+, 30%).

[Ni(2)(SO$_4$)], MX$_n$ = NiSO$_4$·6H$_2$O. Recrystallisation from diethyl ether gave an orange microcrystalline material formulated as [Ni(**2**)(SO$_4$)]·5H$_2$O which decomposed at 270–271 °C (0.210 g, 79%) (Found: C, 51.83; H, 7.50; N, 6.23. Calc. for $C_{38}H_{66}N_4NiO_{13}S$: C, 51.95; H, 7.52; N, 6.38%). δ_H ($CDCl_3$, 200 MHz) 1.26 (s, 9 H, C(CH_3)$_3$), 1.36 (br, 2 H, cyclohexane CH), 1.99 (br, 1 H, cyclohexane CH), 2.50 (br, 1 H, cyclohexane CH), 3.04 (br, 1 H, cyclohexane CH), 2.5–3.5 (br, 4 H, NCH_2CH_2O), 3.7–4.5 (br, 4 H, NCH_2CH_2O), 4.20 (m, 2 H, Ar CH_2N), 7.19 (d, 1 H, *J* 2.4, Ar H), 7.26 (d, 1 H, *J* 2.4 Hz, Ar H) and 7.50 (s, 1 H, N=CH). λ_{max}/nm (CH_2Cl_2) 329, 345, 417 and 460 (sh). $\tilde{\nu}_{max}$/cm^{-1} 1120vs (SO_4). MS (FAB, thioglycerol): *m*/*z* 787 (MH^+, 20%). Diffusion of diethyl ether vapours into a saturated dichloromethane solution produced red plate crystals suitable for X-ray diffraction.

[Ni(1 − 2H)]. This was prepared by using Ni(CH_3CO_2)$_2$·4H$_2$O as the source of nickel in the procedure outlined above. Recrystallisation of the crude product from diethyl ether gave an orange-red microcrystalline material formulated as [Ni(1 − 2H)]·2H$_2$O (0.167 g, 73%), mp 235–240 °C (Found: C, 61.00; H, 7.38; N, 8.19. Calc. for $C_{34}H_{52}N_4NiO_4$: C, 60.77; H, 7.75; N, 8.34%). $\chi_m = 2.47 \times 10^{-10}$ cm^3 mol^{-1}, $\mu_{eff} = 7.6 \times 10^{-4}$ μ_B. δ_H ($CDCl_3$, 200 MHz) 1.24 (m, 9 H, C(CH_3)$_3$), 2.53 (t, 4 H, *J* 4.4, NCH_2CH_2O), 3.35 (s, 2 H, NCH_2CH_2N), 3.61 (s, 2 H, Ar CH_2N), 3.73 (t, 4 H, *J* 4.4, NCH_2CH_2O), 6.89 (d, 1 H, *J* 2.6, Ar H), 7.37 (d, 1 H, *J* 2.6 Hz, Ar H) and 7.46 (s, 1 H, N=CH). λ_{max}/nm (CH_2Cl_2) 324, 346, 417 and 460 (sh). MS (FAB, thioglycerol): *m*/*z* 636 (MH^+, 50%). Diffusing hexane vapours into an ethyl acetate solution of the complex grew single crystals suitable for X-ray diffraction.

Solvent extraction studies

A 0.01 M chloroform solution of ligand **3** (10 cm^3) was intimately mixed with a 1 M aqueous solution of $CuSO_4$ (10 cm^3) at room temperature for 24 h to allow equilibration by which time the solution had turned dark brown. The mixture was allowed to separate and a sample (1 cm^3) of the chloroform solution was removed for ICP-EAS analysis to determine the copper and sulfur content.

Collection and reduction of X-ray data

Data were collected at 220 K on a Stoe 4-circle diffractometer using Mo-Kα radiation ($\lambda = 0.71073$ Å). The structures were solved by direct methods (SHELXS 97)[14] and refined on F^2 by full matrix least squares (SHELXL 97).[15] The quaternary ammonium hydrogen atoms in the structures of [Ni(**1**)(SO$_4$)], [Ni(**1**)(NO$_3$)$_2$] and [Ni(**2**)(SO$_4$)] were located on the difference map and fully refined. All other hydrogen atoms were placed at calculated positions and refined using riding. All non-H atoms

Table 1 Crystallographic data

	2	[Ni(**1** − 2H)]	[Ni(**1**)(SO_4)]	[Ni(**1**)(NO_3)$_2$]	[Ni(**2**)(SO_4)]
Empirical formula	$C_{41}H_{63}N_4O_4$	$C_{34}H_{48}N_4NiO_4$	$C_{37.75}H_{65}N_4NiO_{11.75}S$	$C_{35}H_{52}Cl_2N_6NiO_{10}$	$C_{80}H_{116}ClN_8Ni_2O_{16}S_2$
M	675.95	635.47	518.14	846.44	2052.75
Crystallographic system	Monoclinic	Triclinic	Monoclinic	Monoclinic	Triclinic
Space group	*C*2/*c*	$P\bar{1}$	*P*2/*c*	$P2_1/c$	$P\bar{1}$
a/Å	24.786(3)	7.3052(5)	18.9754(4)	16.5599(16)	11.108(5)
b/Å	12.9082(15)	15.1256(14)	12.8666(3)	14.2742(14)	14.319(7)
c/Å	26.542(4)	15.6704(14)	19.7197(4)	16.7199(16)	16.230(11)
β/°	91.715(18)	87.161(5)	118.571(1)	91.773(7)	107.95(3)
U/Å^3	8488(2)	1631.9(2)	4228.2(2)	3950.3(7)	2368(2)
Z	8	2	4	4	1
μ(Mo-Kα)/mm^{-1}	0.531	0.637	0.571	0.689	0.456
Independent reflections (R_{int})	7339 (0.0593)	6557 (0.1733)	8643 (0.07)	6972 (0.0664)	6928 (0.1161)
No. parameters	434	385	434	506	470
R	0.0720	0.0623	0.0502	0.0519	0.1119
*wR*2	0.2059	0.1362	0.1457	0.1189	0.3271
Largest difference peak and hole/e Å^{-3}	0.237 and −0.209	0.494 and −0.438	1.234 and −0.669	0.277 and −0.282	0.577 and −0.442

were modelled with anisotropic displacement parameters and final refinement statistics are presented in Table 1.

CCDC reference number 186/2020.

See http://www.rsc.org/suppdata/dt/b0/b003436n/ for crystallographic files in .cif format.

Results and discussion

Synthesis of new Schiff base ligands

The Schiff base ligands were readily prepared by a four-step convergent synthesis (Scheme 3) from a substituted salicylaldehyde, paraformaldehyde, morpholine and a diamine of choice. The preferred method of preparation of the substituted salicylaldehydes was based upon the industrial process developed by Levin and co-workers[12] involving magnesium-mediated formylation using magnesium methoxide and paraformaldehyde. Subsequent substitution in the remaining *ortho* position with the morpholinomethyl group was achieved *via* a Mannich reaction[13] under non-aqueous aprotic conditions. The Mannich base ethoxymorpholinomethane was prepared[13] from morpholine and paraformaldehyde in ethanol with potassium carbonate and purified by distillation. The Schiff base condensations of the substituted salicylaldehydes with appropriate diamines were undertaken at room temperature in non-aqueous solvents. Each ligand has been characterised by ^{1}H and ^{13}C NMR spectroscopy, FAB mass spectrometry and elemental analysis.

"Free" ligand structures

Single crystals of ligand **2** suitable for structure determination were grown by evaporation of a CH_2Cl_2 solution. The molecule (Fig. 3) adopts a *trans* configuration with a pseudo twofold rotation axis bisecting the cyclohexane unit. The *trans* configuration is similar to that found[17] in the solid state structures of a number of similar H_2salen ligands. The tertiary butyl groups are disordered with about two sites of approximately equal occupancy.

During the course of this work, Shanmuga *et al.*[18] published the structure of ligand **4**, which is similar to **1**, having two pendant morpholine groups, but with the tertiary butyl groups replaced by methyls. The molecule adopts a fully extended conformation with an N–C–C–N torsion angle of 180° in the central ethane bridge and a distance of 8.19 Å between the phenolic oxygen atoms. The morpholine rings are also well separated, with a morpholine N ··· N distance of 16.22 Å.

By comparison, the rigid 1,2-cyclohexane bridging group of compound **2** constrains the ligand to a configuration better predisposed to metal complexation by bringing the [N_2O_2] donor set into closer proximity. The torsion angle N(2A)–C(22A)–C(22B)–N(2B) is 63.1° and the phenolic oxygens

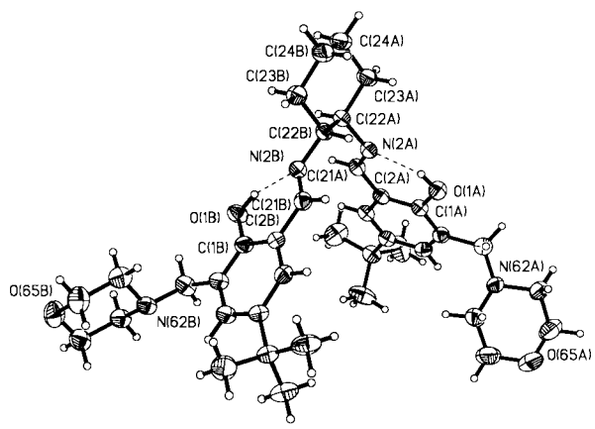

Fig. 3 An ORTEP[16] plot (30% probability ellipsoids) of ligand **2** showing the pseudo C_2 rotation axis relating the halves of the ligand A and B. Selected bond lengths (Å); C(22A)–N(2A), 1.460(4), C(21A)–N(2A), 1.271(4), C(22B)–N(2B), 1.460(4), C(21B)–N(2B), 1.271(4), C(21A)–C(2A), 1.452(4), C(21B)–C(2B), 1.454(4), C(1A)–O(1A), 1.359(3), C(1B)–O(1B), 1.364(4). Intramolecular distances between nitrogen and oxygen atoms (Å); N(2A) ··· O(1A) 2.635 and N(2B) ··· O(1B) 2.604.

O(1A) and O(1B) are separated by 6.53 Å. The dihedral angle of 95.3° between the benzene rings of **2** suggests a predisposition for tetrahedral co-ordination geometry. However, the distance between the phenolic oxygen donors is large compared with that needed to define adjacent sites at a metal ion. The 1,2-cyclohexane bridge constrains the two pendant morpholine groups to be closer together (N(62A) ··· N(62B) 11.77 Å) than in the ethane bridged ligand **4**.

Neither of these ligands in their metal-free or "at rest" state has a geometry preorganised for either cation or anion binding. To bring the morpholine rings into close proximity to encapsulate an anion requires a major change to the geometry of the ligand backbone. The extent to which incorporation of a metal cation into the salen donor set "templates" the creation of an anion binding site is considered below. The preorganisation of ligands for anion binding by incorporation of metals into the system has previously been reported.[19] The novelty of the ligands **1**–**3** is the concomitant creation of an electrostatic binding site for the anion (see below).

Formation of metal salt complexes

Nickel(II) was selected for study of the binding of metal salts by the ditopic ligands **1** and **2** on the grounds that it readily forms low spin diamagnetic planar complexes with H_2salen-type ligands and that these can conveniently be studied by ^{1}H NMR

Table 2 Electronic absorption spectra of ligands **1** and **2** and their complexes of Ni^{II} and Cu^{II}

Compound	λ_{max}/nm
1	235, 262, 329, 413
2	234, 261, 328, 417
[Ni(**1** − 2H)]	324, 346, 417, 460 (sh)
[Ni(**1**)(SO_4)]	328, 339, 418, 460 (sh)
[Ni(**1**)(NO_3)$_2$]	327, 339, 415, 460 (sh)
[Ni(**2**)(SO_4)]	329, 345, 417, 460 (sh)
[Cu(**1**)(SO_4)]	371, 557

spectroscopy. The formation of the nickel(II) sulfate complexes occurs almost immediately upon mixing in alcoholic solution. Elemental analysis and FAB mass spectrometry confirm the formation of 1 : 1 : 1 nickel : ligand : sulfate assemblies in the solid state. When nickel(II) nitrate is used the dinitrato complex [Ni(**1**)(NO_3)$_2$] is obtained. Copper(II) sulfate complexes are also readily prepared in a similar manner. In this paper we include only the one copper complex, [Cu(**1**)(SO_4)], the characteristic of which relates to solvent extraction data (see below). Characteristic absorbances for the sulfate and nitrate anions were observed in the IR spectra of these complexes.

The basicity of the counter ion is important in determining the outcome of the complexation reactions. When nickel(II) acetate is used as the metal source there is no evidence for the presence of the attendant anion in the product. The formation of [Ni(**1** − 2H)] follows the norm for H_2salen-type ligands, presumably because acetate effectively competes with the morpholine nitrogen atoms for the protons released by the phenolic groups.[20] The ability to prepare neutral complexes of either a metal dication or its salts is very unusual and could have important consequences in developing protocols to deal with the loading and stripping in solvent extraction processes (see below).

Electronic absorption spectroscopy

The electronic absorption spectra of ligands **1** and **2** consist of a set of three intense bands at 235, 262 and 329 nm involving $\pi \longrightarrow \pi^*$ transitions and a low intensity feature in the 410–420 nm region involving $n \longrightarrow \pi^*$ excitation (Table 2).[21] The colour changes due to metal complexation follow those expected for H_2salen type complexes of these metals, *i.e.* red-orange for Ni^{II} and dark brown for Cu^{II}. Metallation with nickel results in two overlapping features assigned to two different types of transitions. A broad band in the region 300–360 nm involves intraligand $\pi \longrightarrow \pi^*$ transitions and a new set of absorbances in the 380–460 nm region with charge transfer character. A weak feature assigned to d–d transitions is present in the 500–600 nm region.[22] Changes in the spectra upon copper complexation are less dramatic. An intense mixture of $\pi \longrightarrow \pi^*$ and $n \longrightarrow \pi^*$ ligand based transitions occurs at around 370 nm. A weak asymmetric broad band in the visible region around 550 nm can be assigned to d–d transitions.[23,24]

A comparison of the spectrum of the "nickel only" complex with those of the nickel salt complexes indicates that the effect of anion binding upon the electronic absorption spectra of these complexes is minimal. This suggests that the cation and anion binding sites are well separated in these assemblies in solution and that the anions do not interact strongly with the metal-based chromophore. This observation is supported by NMR and solid state structural studies (see below).

^{1}H NMR spectra of the nickel(II) complexes

The ^{1}H NMR spectra of the nickel(II) complexes were recorded at 200 MHz in $CDCl_3$ at room temperature. Complexes of ligand **1** were shown to be diamagnetic with no solid state room temperature magnetic moment, consistent with square planar co-ordination which was confirmed by X-ray crystallography (see below). The NMR spectra showed no evidence of paramagnetic line broadening or shifts suggesting the square planar geometry existing in the solid state is retained in $CDCl_3$ solution and that there is no strong interaction with the anions in axial co-ordination sites. Metallation with nickel shifts signals of protons close to the co-ordination site to lower frequency relative to those of the "free" ligand and the phenolic proton signal is lost consistent with metal incorporation into an $[N_2O_2]^{2-}$ donor set. Data for the azomethine group and bridging methylene groups are shown in Table 3.

Table 3 Shift in ligand proton resonances upon complexation ($\Delta\delta$ (ppm), 200 MHz, $CDCl_3$)

Compound	N=C*H*	NCH_2CH_2N	Ar CH_2N
[Ni(**1** − 2H)]	−0.91	−0.23	−0.29
[Ni(**1**)(SO_4)]	−0.70	−0.09	+0.4
[Ni(**1**)(NO_3)$_2$]	−0.72	−0.13	+0.33
[Ni(**2**)(SO_4)]	−0.77	—	+0.66

A comparison of the spectra of [Ni(**1** − 2H)] with those of the salt complexes [Ni(**1**)(SO_4)], [Ni(**1**)(NO_3)$_2$] and [Ni(**2**)(SO_4)] in regions associated with the pendant morpholine groups provides evidence for the protonation of the tertiary nitrogens and their bonding to the attendant anions in solution. The Ar CH_2N methylene signal of [Ni(**1** − 2H)] is shifted upfield relative to the "free" ligand to a similar extent to those of methylene groups linking the azomethine nitrogen atoms (Table 3). In contrast, in the salt complexes protonation of the tertiary amine nitrogens shifts the Ar CH_2N methylene signals downfield (Table 3). Also, unlike [Ni(**1** − 2H)], for the salt complexes both the morpholine methylene resonances are broadened and can only just be seen above the baseline. Association of the anions with the morpholinium rings appears to reduce ring flexibility and lowers their symmetry. Protonation of the morpholine nitrogen also reduces the overall symmetry in addition to slowing the rate of ring conformation inversion.

Metal salt extraction experiments

Some preliminary solvent extraction experiments have been carried out to establish proof-of-concept of transporting metal sulfates in water immiscible solvents. For these experiments copper sulfate was used as the kinetics of phase transfer of nickel salts was found to be very slow in comparison and much longer equilibration times are needed. Close to 100% extraction of copper and sulfate into a chloroform solution of lipophilic ligand **3** was observed on contacting an aqueous $CuSO_4$ solution (1 M) at pH 3.8.[24] Analysis of the loaded organic solution indicates that copper sulfate has been accommodated as discrete 1 : 1 : 1 copper : ligand : sulfate packages. Development of the stripping protocols for copper and sulfate have required tuning down the "strength" of the metal binding site to facilitate the removal of copper prior to recovery of the sulfate as in Scheme 1. The development of lipophilic ligands with selectivities and strengths to affect recovery of specific metals will be described in forthcoming papers. In the section below solid state structures of nickel complexes are used to define modes of anion binding and consider the co-operativity of Ni^{2+} and anion complexation.

X-Ray crystallography

The crystal structure of [Ni(**1** − 2H)] confirms the absence of any associated anions (Fig. 4). The approximately planar [Ni(salen)] components stack "back to front" about the inversion centre with azomethine H to adjacent phenyl ring distances of approximately 3.8 Å and a weak C–H · · · N intermolecular hydrogen bond between one of the tertiary amine nitrogens and a bridging methylene hydrogen (H(22C) · · · N(62A) 2.51 Å with

Table 4 Bond lengths (Å) and angles (°) in the co-ordination spheres of [Ni(**1** − 2H)], [Ni(**1**)(SO_4)] and [Ni(**1**)(NO_3)$_2$]

	[Ni(**1** − 2H)]		[Ni(**1**)(SO_4)]		[Ni(**1**)(NO_3)$_2$]	
	Part A[a]	Part B[b]	Part A	Part B	Part A	Part B
Ni(1)–N(2)	1.834(3)	1.838(3)	1.846(2)	1.858(2)	1.852(3)	1.852(3)
Ni(1)–O(1)	1.849(2)	1.844(3)	1.848(2)	1.854(2)	1.859(3)	1.855(2)
O(1)–Ni(1)–N(2)	94.77(13)	94.42(13)	93.67(8)	94.51(8)	94.16(12)	94.38(12)
O(1)–Ni(1)–O(1)′[b]	84.92(11)	—	85.90(7)	—	86.38(11)	—
N(2)–Ni(1)–N(2)	86.22(14)	—	85.97(9)	—	85.73(13)	—
O(1)–Ni(1)–N(2)′	175.46(12)	—	177.20(8)	—	173.36(14)	—
N(2)–Ni(1)–O(1)′	175.75(12)	—	178.86(9)	—	174.40(13)	—
Σ *cis*-angles	360.3(5)	—	360.1(3)	—	360.7(5)	—
N(2)–C(22)–C(22)′–N(2)′ torsion	12.3	—	38.3	—	42.4	—
Inclinations (°) between the least squares plane of the N_2O_2 donor set and the N(2)–C(2)–C(3)–C(22)–O(1) chelate rings						
	4.0	9.1	16.9	1.1	−10.6	7.6
Displacement of morpholine ring atoms (Å) from least squares plane of the N_2O_2 donor set						
N(62)	0.806	1.672	1.559	−1.250	0.138	2.121
O(65)	2.286	3.825	4.168	−4.065	2.091	4.225

[a] Parts A and B refer to the chemically equivalent halves of the ligand (see figures for definitions of atom labels). [b] The prime refers to the chemically equivalent atom in part B of the ligand.

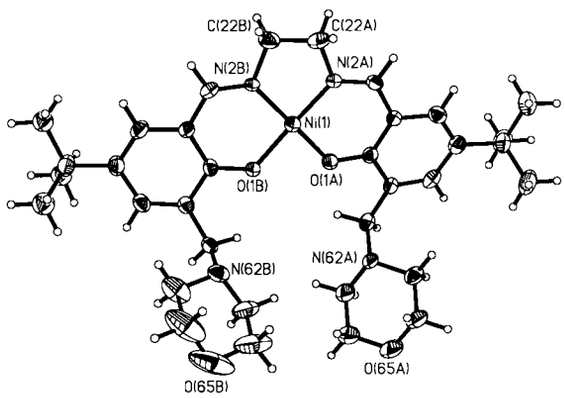

Fig. 4 An ORTEP plot (50% probability ellipsoids, as in all structures shown) of the molecular structure of [Ni(**1** − 2H)].

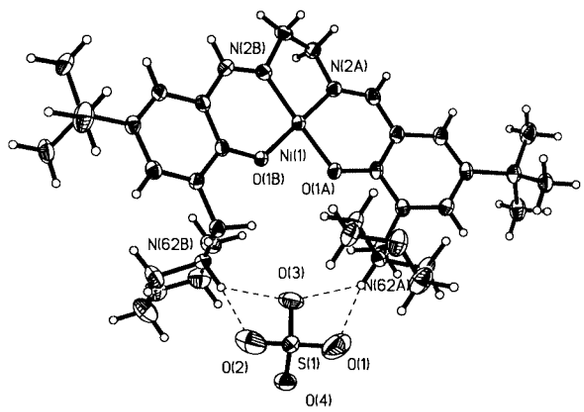

Fig. 5 An ORTEP plot of the molecular structure of [Ni(**1**)(SO_4)].

C(22B)–H(22C)···N(62A) 158.4°). The planar NiN_2O_2 unit has bond lengths and angles typical[26] for [Ni(salen)] type complexes (Table 4). The sum of chelating angles around the nickel is 360.3(5)°.

The co-ordination of Ni^{2+} to the $[N_2O_2]^{2-}$ donor set has a major effect on the conformation of the ligand and, in particular, the disposition of the pendant morpholine groups. The bridging ethane-1,2-diamine torsion angle is reduced from 180° in **4** to 12.3° and the benzene rings are rotated through almost 180° to bring the morpholine groups into proximity; the morpholine N···N separation in [Ni(**1** − 2H)] is 5.17 Å, while the "free" ligand **4** has a morpholine N···N distance of 16.22 Å. The structure determination confirms that the planar nickel(II) centre templates the ligand to create a potential anion-binding cavity between the two protonatable morpholine rings. Incorporation of a dianion into this dicationic cavity will generate a charge-neutral entity with a relatively lipophilic exterior, increasing the overall solubility of the package in non-polar solvents, an important feature for solvent extraction purposes. The two morpholine groups are also likely to hydrogen-bond strongly to any incorporated anion.

The structure determination of [Ni(**1**)(SO_4)] (Fig. 5) demonstrates how a combination of preorganisation of the ligand by nickel(II) for anion binding and transformation of the ligand into its zwitterionic form are key to the strong metal salt binding. The geometry of the metal co-ordination sphere (see Table 4) is very similar to that in [Ni(**1** − 2H)] and other[26] [Ni(salen)] type complexes and only small variations in chelate bite angles accompany the incorporation of the anion in the morpholine binding site (see below). The protons formally transferred from the phenolic oxygens to the morpholine nitrogen atoms were detected in the difference map (largest peak is 1.234 e $Å^{-3}$, deepest hole is −0.669 e $Å^{-3}$). The sulfate anion is bound in the resulting dipositive cavity by a combination of electrostatic interactions and two bifurcated N–H···O hydrogen bonds (Table 5). The amine protons are orientated inwards, towards the cavity occupied by the sulfate, giving an N···N separation of 5.16 Å.

The shortest nickel–sulfate contact distance (Ni···O 5.44 Å) is too large for there to be any strong interaction between the anion and the Lewis acidic metal centre. Such an arrangement contrasts with the uranylsalen anion receptor of Reinhoudt and co-workers[28] which has been shown to bind $H_2PO_4^-$ *via* a combination of two N-H···O (non-charge assisted) hydrogen bonds and a single co-ordinate bond between a phosphate oxygen and the uranyl metal centre.

In [Ni(**1**)(SO_4)] the incorporation of the sulfate between the morpholinium groups is associated with changes in the conformation of the ligand framework. The morpholine rings are located on opposite sides of the NiN_2O_2 plane and the ligand backbone experiences a slight twist with an increase in both the bridging ethane-1,2-diamine torsion angle and dihedral angle between the benzene rings (Table 4). The nickel co-ordinate

Table 5 Hydrogen bonded distances (Å) and angles (°) around the sulfate anion in [Ni(**1**)(SO_4)]

	N···O	N–H···O	H···O
O1···H(62A)–N(62A)	2.870(4)	166.2	1.958
O2···H(62B)–N(62B)	2.923(3)	154.1	2.322
O3···H(62A)–N(62A)	2.993(4)	128.8	2.058
O3···H(62B)–N(62B)	2.915(4)	132.1	2.209

Note: the N–H distances were fixed at 0.91 Å. Hydrogen bonds were assigned using the PLATON program[27] to interactions of the oxygen and nitrogen atoms that were <3.12 Å.

Table 6 Hydrogen bonded distances (Å) and angles (°) around the nitrate anions in [Ni(**1**)(NO_3)$_2$]

	N···O	N–H···O	H···O
O(1S1)···H(62A)–N(62A)	2.906	137.30	2.116
O(1S2)···H(62A)–N(62A)	2.938	160.24	2.005
O(2S1)···H(62B)–N(62B)	3.306	129.00	2.619
O(2S3)···H(62B)–N(62B)	2.760	171.38	1.811

Details as in Table 5.

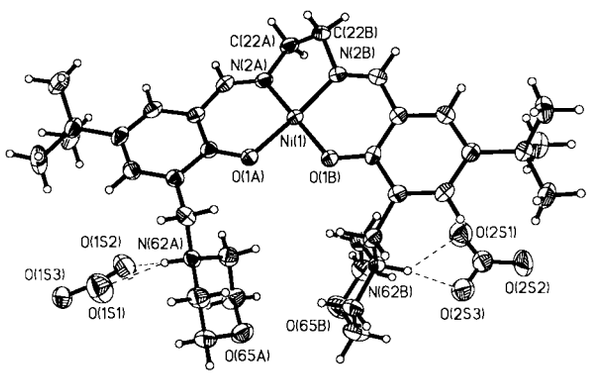

Fig. 6 An ORTEP plot of the molecular structure of [Ni(**1**)(NO_3)$_2$].

bonds are not significantly changed and the square planar geometry is retained. To accommodate this the ligand experiences a slight splaying with a smaller N(2)–Ni–N(2′) angle and a larger O(1)–Ni–O(1)′ angle. The accommodation of the anion between the morpholinium groups is facilitated by the flexibility of the methylene linkages which allow various conformations to be adopted as demonstrated by this set of structures.

The solid state structure of [Ni(**1**)(NO_3)$_2$] indicates that both nitrates are bound to the complex unit (Fig. 6) by a combination of electrostatic and bifurcated N–H···O hydrogen bonds to the morpholinium amine protons (Table 6). In contrast to the sulfate complex the nitrate anions are bound outside of the cavity formed by the morpholine rings, and the quaternary protons point away from each other. The morpholine rings are arranged on the same side of the plane described by the NiN_2O_2 complex in a folded arrangement similar to that in [Ni(**1** − 2H)] whereas in the sulfate structure they sit on opposite sides with a pseudo C_2 rotation axis. One of the tertiary butyl groups is disordered about two sites of approximately equal occupancy.

A comparison of the [Ni(**1**)(SO_4)], [Ni(**1**)(NO_3)$_2$] and [Ni(**1** − 2H)] structures suggests that incorporation of the sulfate into the morpholinium binding site has a smaller effect on the nickel co-ordination geometry than accommodation of the two nitrates. The N–C–C–N torsion angle of the ethane bridge in [Ni(**1**)(NO_3)$_2$] is increased, and while the co-ordinate bonds around the square planar nickel are not significantly different from the other nickel complexes, the ligand is splayed with a smaller N(2)–Ni–N(2)′ angle and a larger O(1)–Ni–O(1)′ angle (Table 4). It appears that the templating of the ligand **1** by co-ordination to nickel(II) generates a system which is well

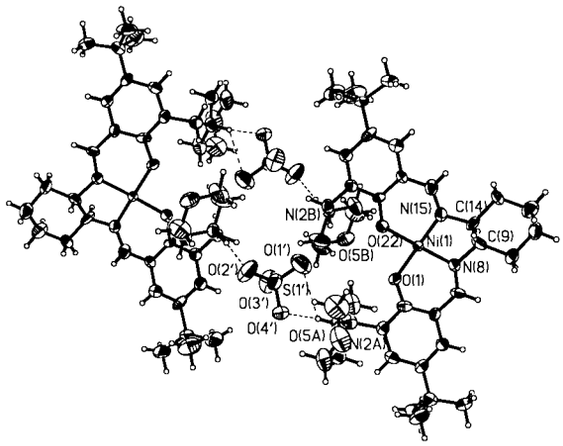

Fig. 7 An ORTEP plot of the molecular structure of [Ni(**2**)(SO_4)]. Selected bond lengths (Å) and angles (°); Ni(1)–N(15) 1.824(8), Ni(1)–N(8) 1.859(7), Ni(1)–O(22) 1.832(6) and Ni(1)–O(1) 1.854(6); O(22)–Ni(1)–N(15) 94.9(3), O(1)–Ni(1)–N(8) 94.6(3), O(22)–Ni(1)–O(1) 85.2(3) and N(15)–Ni(1)–N(8) 86.2(3).

suited to sulfate binding because there are only very minor changes to the nickel geometry when the sulfate ion is incorporated (compare [Ni(**1** − 2H)] and [Ni(**1**)(SO_4)] in Table 4). Such co-operativity of cation/anion binding will have an important consequence on the selectivity of recovery of metal salts by solvent extraction. The geometric interplay between the cation and anion binding sites will also influence the external structure of the package. More favourable distribution coefficients for extraction of metal salts into the hydrocarbon solvents preferred for industrial use are likely to be observed when the polar cation and anion components in the overall charge-neutral complex are shielded from the solvent by hydrophobic substituents. Work is in hand to adapt the prototype ligands described here to achieve this.

Extended supramolecular assemblies

The formation of these simple supramolecular metal salt assemblies led us to envisage the possibility of building up three-dimensional arrays of metal cations using the cationic binding sites in conjunction with various bridging anions. The incorporation of metal ions into hydrogen-bonded arrays has recently received attention as such systems may have interesting magnetic, optical and conductivity properties.[29] The structure of [Ni(**1**)(NO_3)$_2$] showed the nitrate anions bound on the outside of the morpholine cavity which although undesirable for solvent extraction purposes demonstrates that anions could perhaps bridge between two ligands. Such an arrangement is found in the structure of [Ni(**2**)(SO_4)] (Fig. 7). Two nickel complexes of the 1,2-cyclohexane bridged ligand **2,** related by an inversion centre, are linked into a pseudo macrocycle by two bridging sulfate anions *via* a combination of electrostatic interactions and intermolecular N–H···O hydrogen bonds (Table 7). The nickel bond lengths and angles are not significantly different from those of the nickel complexes of ligand **1** despite the fact that the rigid 1,2-cyclohexane unit fixes the bridging torsion angle closer to that of the "free" ligand (N(15)–C(14)–C(9)–N(8) 51.8°, "free" ligand 63.1°).

The pendant morpholine rings are arranged on opposite sides of the plane of the nickel salen complex creating the same pseudo C_2 symmetry as that of [Ni(**1**)(SO_4)]. The two sulfate anions are bound to the morpholinium amine protons, one by a single N–H···O hydrogen bond and the other by a bifurcated N–H···O hydrogen bond (Table 7). The sulfates are bound facially to the morpholine rings so that they can form additional hydrogen bonds to the morpholine quaternary amine protons of the opposing ligand. In total each sulfate forms one single hydrogen bond and one bifurcated hydrogen bond.

Table 7 Hydrogen bonded distances (Å) and angles (°) around the sulfate anion in [Ni(**2**)(SO_4)]

	N···O	N–H···O	H···O
O(1)′···H(2A)–N(2A)	3.165	123.1	2.568
O(4)′···H(2A)–N(2A)	2.609	173.0	1.693
O(2)′···H(2B)–N(2B)	2.646	171.4	1.732

Note: the N–H distances were fixed at 0.92 Å. Other details as in Table 5.

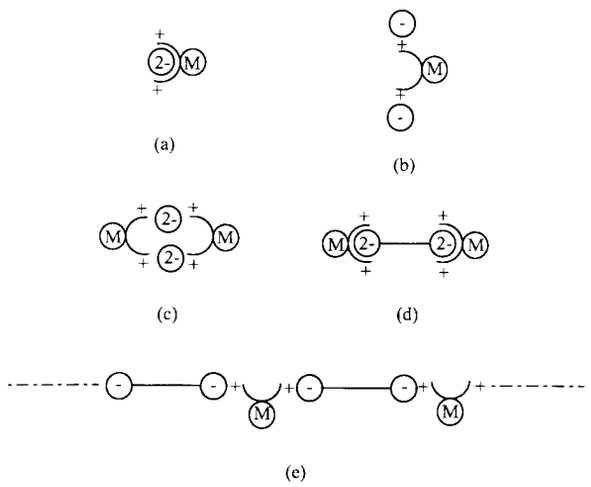

Fig. 8 Supramolecular assemblies of metal salts with ditopic ligands. Motifs **a**, **b** and **c** are observed in the structures of [Ni(**1**)(SO_4)], [Ni(**1**)(NO_3)$_2$] and [Ni(**2**)(SO_4)] respectively. Assemblies **d** and **e** are proposed using the rigid polyacids (4-phosphonophenyl)phosphonic acid and terephthalic acid respectively.

The observation that anions are able to bridge two ligands *via* intermolecular charge-assisted hydrogen bonding presents us with the opportunity to design two- or three-dimensional supramolecular assemblies. To develop strategies for building up arrangements of molecular building blocks requires that they be rigid with a suitable supramolecular *synthons*, *e.g.* a set of complementary hydrogen bond donors and acceptors, such that the resulting architectures are predictable and reproducible.[30] Preorganisation of ditopic ligands similar to **1**–**4** by binding different metals to create molecules with particular dispositions of the anion binding sites should facilitate their use in this way. The three types of simple metal salt assemblies obtained so far are represented schematically as **a**–**c** in Fig. 8. Each pendant morpholinium quaternary amine group represents a single *hydrogen bond donor*, which can bind by a combination of electrostatic and hydrogen bonding to a range of anions. The electrostatic component is largely non-directional providing the "glue" for the interaction whereas the hydrogen bonds provide the directional element, allowing the linking together of ions in a predictable manner.

Rigid polyanions such as terephthalate and (4-phosphonophenyl)phosphonate provide anionic *hydrogen bond acceptors* with predictable bonding properties. Terephthalic acid has been used to link metal complexes into extended supramolecular tapes and sheets.[31,32] A combination of these anionic hydrogen bond acceptor synthons with the cationic hydrogen bond donor sites of our complexes would be expected to generate oligomeric systems, such as **e** or two or three dimensional lattices depending on the level of multifunctionality in the anion and/or cation (Fig. 9). Work is in hand using (4-phosphonophenyl)phosphonic acid to bridge the metal complexes in dumbbell assemblies (**d**) and terephthalic acid to form extended sheets or ribbons (**e**). Assembly is effected by addition of the polyacid to preformed neutral metal complexes such as [Ni(**1** − 2H)], *etc*.

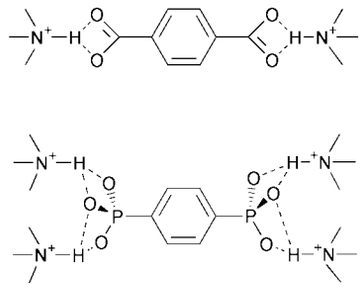

Fig. 9 Proposed mode of hydrogen bond formation between the rigid polyacids terephthalic acid and (4-phosphonophenyl)phosphonic acid and quaternary ammonium protons.

Conclusions

We have used relatively simple ditopic ligands related to H_2salen to establish the proof-of-concept of selective transportation of metal sulfates under conditions which would allow the development of novel flowsheets for hydrometallurgical processing of sulfidic ores. The accommodation of the metal sulfate into a zwitterionic form of the ditopic ligand ensures that the complexed package is charge neutral permitting transfer into non-polar water immiscible solvents suitable for solvent extraction and can effectively be stripped to generate an electrolyte suitable for metal recovery. These design features, coupled with the ability to tailor the selectivity of the metal cation binding site, would form the basis for the unit operations of "separation" and "reduction" in an industrial process, generating an electrolyte with a suitable purity to effect "reduction". Commercial viability will depend on developing ligands which show stability to hydrolysis and oxidation and good kinetics of metal transport under operating conditions.

The design of prototype extractants has been based on principles of supramolecular chemistry which should also allow assembly of unusual solid state materials.

Acknowledgements

We thank Mr J. Millar and Mr W. Kerr for obtaining NMR spectra, Mr A. Taylor and Mr H. Mackenzie for mass spectra and Ms L. Eades for elemental analysis. We gratefully acknowledge the EPSRC for a ROPA award (GRM/33303) and Avecia (formerly Zeneca Specialties) for funding.

Notes and references

1 D. S. Flett, *Hydrometallurgy*, 1992, **30**, 327.
2 J. Szymanowski, in *Hydroxyoximes and Copper Hydrometallurgy*, CRC Press, Boca Raton, FL, 1993, p. 62.
3 For reviews of anion recognition: B. Dietrich, *Pure Appl. Chem.*, 1993, **65**, 1457; C. Seel and J. de Mendoza, in *Comprehensive Supramolecular Chemistry*, eds. J. L. Atwood, J. E. D. Davies, D. D. MacNicol and F. Vogle, Elsevier Science Ltd, Oxford, 1996, pp. 519–552; A. Bianchi, K. Bowman-James and E. Garcia-España (Editors), *Supramolecular Chemistry of Anions*, Wiley-VCH, New York, 1997; F. P. Schmidtchen and M. Berger, *Chem. Rev.*, 1997, **97**, 1609; M. M. G. Antonisse and D. N. Reinhoudt, *Chem. Commun.*, 1998, 443.
4 B. C. Hamann, N. R. Branda and J. Rebek, Jr., *Tetrahedron Lett.*, 1993, **34**, 6837; T. R. Kelly and M. H. Kim, *J. Am. Chem. Soc.*, 1994, **116**, 7072; S. Nishizawa, P. Bühlmann, M. Iwao and Y. Umezawa, *Tetrahedron Lett.*, 1995, **36**, 6483; C. Bazzicalupi, A. Bencini, A. Bianchi, M. Cecchi, B. Escuder, V. Fusi, E. Garcia-España, C. Giorgi, S. V. Luis, G. Maccagni, V. Marcelino, P. Paoletti and B. Valtancoli, *J. Am. Chem. Soc.*, 1999, **121**, 6807.
5 For metal salt binding ditopic receptors: U. Olsher, F. Frolow, N. K. Dalley, J. Weiming, Z.-Y. Yu, J. M. Knobeloch and R. A. Bartsch, *J. Am. Chem. Soc.*, 1991, **113**, 6570; E. A. Arafa, K. I. Kinnear and J. C. Lockhart, *J. Chem. Soc., Chem. Commun.*, 1992, 61; P. J. Smith, M. V. Reddington and C. S. Wilcox, *Tetrahedron Lett.*, 1992, **33**, 6085; S. S. Flack, J.-L. Chaumette, J. D. Kilburn, G. J. Langley and M. Webster, *J. Chem. Soc., Chem. Commun.*, 1993, 399; P. B. Savage, S. K. Holmgren and S. H. Gellman, *J. Am. Chem.*

Soc., 1994, **116**, 4069; M. T. Reetz, in *Comprehensive Supramolecular Chemistry*, eds. J. L. Atwood, J. E. D. Davies, D. D. MacNicol and F. Vogle, Elsevier Science Ltd, Oxford, 1996, pp. 553–563; N. Pelizzi, A. Casnati, A. Friggeri and R. Ungaro, *J. Chem. Soc., Perkin Trans. 2*, 1998, 1307; P. D. Beer and J. B. Cooper, *Chem. Commun.*, 1998, 129.
6 P. D. Beer and D. K. Smith, *Prog. Inorg. Chem.*, 1997, **46**, 1 and references therein.
7 P. D. Beer, P. K. Hopkins and J. D. McKinney, *Chem. Commun.*, 1999, 1253.
8 K. Kavallieratos, R. A. Sachleben, G. J. Van Berkel and B. A. Moyer, *Chem. Commun.*, 2000, 187.
9 L. A. J. Chrisstoffels, F. de Jong, D. N. Reinhoudt, S. Sivelli, L. Gazzola, A. Casnati and R. Ungaro, *J. Am. Chem. Soc.*, 1999, **121**, 10142.
10 D. J. White, N. Laing, H. Miller, S. Parsons, S. Coles and P. A. Tasker, *Chem. Commun.*, 1999, 2077; P. A. Tasker and D. J. White, *Br. Pat.*, 9907485.8, 1999.
11 E. A. Boudreaux and C. N. Mulay, *Theory and Applications of Molecular Paramagnetism*, Wiley, London, 1976.
12 R. Aldred, R. Johnston, D. Levin and J. Neilan, *J. Chem. Soc., Perkin Trans. 1*, 1994, 1823.
13 H. Adams, N. A. Bailey, D. E. Fenton and G. Papageorgiou, *J. Chem. Soc., Dalton Trans.*, 1995, 1883.
14 SHELXS 97, G. M. Sheldrick, University of Göttingen, 1997.
15 SHELXL 97, G. M. Sheldrick, University of Göttingen, 1997.
16 C. K. Johnson, ORTEP II, Report ORNL-5138, Oak Ridge National Laboratory, Oak Ridge, TN, 1976.
17 K. Bernardo, S. Leppard, A. Robert, G. Commenges, F. Dahan and B. Meunier, *Inorg. Chem.*, 1996, **35**, 387.
18 S. Shanmuga, S. Raj, R. Thirumurugan, G. Shanmugam, H.-K. Fun, J. Manonmani and M. Kandaswamy, *Acta Crystallogr., Sect. C*, 1999, **55**, 94.
19 K. Araki, S. K. Lee, J. Otsuki and M. Seno, *Chemistry Lett.*, 1993, 493; P. D. Beer, *Chem. Commun.*, 1996, 689; M. J. Deetz and B. D. Smith, *Tetrahedron Lett.*, 1998, **39**, 6841.
20 Comparison of the pK_a of HSO_4^- (1.92), HNO_3 (3.37) and CH_3CO_2H (4.75) with the values for a range of *N*-alkyl substituted morpholine derivatives (pK_a 6–7) suggests a combination of relative pK_a and solution conditions determines whether the anion or morpholine nitrogen will bind the liberated protons. P. W. Atkins, *Physical Chemistry 5th Edition*, Oxford University Press, Oxford, 1994; D. D. Perrin, *Dissociation Constants of Organic Bases in Aqueous Solutions*, Butterworth & Co., London, 1965.
21 S. M. Crawford, *Spectrochim. Acta*, 1963, **19**, 255.
22 S. Di Bella, I. Fragala, I. Ledoux, M. A. Diaz-Garcia and T. J. Marks, *J. Am. Chem. Soc.*, 1997, **119**, 9550.
23 M. M. Bhadhade and D. Srinivas, *Inorg. Chem.*, 1993, **32**, 5458.
24 S. Koner, *Chem. Commun.*, 1998, **5**, 593.
25 A crystal structure of [Cu(**1**)(SO_4)] has been obtained which shows the copper ion bound in a square planar geometry to the $[N_2O_2]^{2-}$ donor set with bond lengths and angles typical of copper bound to H_2salen type ligands. The sulfate anion is bound between the morpholine rings electrostatically and by two N–H · · · O hydrogen bonds to the quaternary amine protons. The metal salt binding in this structure is analogous to that described in this paper for [Ni(**1**)(SO_4)]. The structure of [Cu(**1**)(SO_4)] will be reported in full in a subsequent publication.
26 A survey of the CCDC reveals 66 square planar nickel(II) salen complexes. Ni–N and Ni–O distances average 1.86 and 1.85 Å respectively. D. A. Fletcher, R. F. McMeeking and D. J. Parkin, *J. Chem. Inf. Comput. Sci.*, 1996, **36**, 746.
27 P. van der Sluis and A. L. Spek, *Acta Crystallogr., Sect. A*, 1990, **46**, 34, 194.
28 D. M. Rudkevich, Z. Brzozka, M. Palys, H. C. Visser, W. Verboom and D. N. Reinhoudt, *Angew. Chem., Int. Ed. Engl.*, 1994, **33**, 467.
29 D. Braga, F. Grepioni and G. R. Desiraju, *Chem. Rev.*, 1998, **98**, 1375; R. Vilar, M. P. Mingos, A. J. P. White and D. J. Williams, *Angew. Chem., Int. Ed.*, 1998, 37, 1258; M. M. Chowdhry, M. P. Mingos, A. J. P. White and D. J. Williams, *Chem. Commun.*, 1996, 899; A. D. Burrows, C.-W. Chan, M. M. Chowdry, J. E. McGrady and D. M. P. Mingos, *Chem. Soc. Rev.*, 1995, **24**, 329.
30 C. B. Aakeröy, *Acta Crystallogr., Sect. B*, 1997, **53**, 569.
31 E. Kimura, T. Ikeda, M. Shionoya and M. Shiro, *Angew. Chem., Int. Ed. Engl.*, 1995, **34**, 663.
32 A. D. Burrows, D. M. P. Mingos, A. J. P. White and D. J. Williams, *Chem. Commun.*, 1996, 97.